nature medicine

Cold-inducible RNA-binding protein (CIRP) triggers inflammatory responses in hemorrhagic shock and sepsis

Xiaoling Qiang[1,4], Weng-Lang Yang[1,4], Rongqian Wu[1], Mian Zhou[1], Asha Jacob[1], Weifeng Dong[1], Michael Kuncewitch[1], Youxin Ji[1], Huan Yang[2], Haichao Wang[2], Jun Fujita[3], Jeffrey Nicastro[1], Gene F Coppa[1], Kevin J Tracey[2] & Ping Wang[1]

A systemic inflammatory response is observed in patients undergoing hemorrhagic shock and sepsis. Here we report increased levels of cold-inducible RNA-binding protein (CIRP) in the blood of individuals admitted to the surgical intensive care unit with hemorrhagic shock. In animal models of hemorrhage and sepsis, CIRP is upregulated in the heart and liver and released into the circulation. In macrophages under hypoxic stress, CIRP translocates from the nucleus to the cytosol and is released. Recombinant CIRP stimulates the release of tumor necrosis factor-α (TNF-α) and HMGB1 from macrophages and induces inflammatory responses and causes tissue injury when injected *in vivo*. Hemorrhage-induced TNF-α and HMGB1 release and lethality were reduced in CIRP-deficient mice. Blockade of CIRP using antisera to CIRP attenuated inflammatory cytokine release and mortality after hemorrhage and sepsis. The activity of extracellular CIRP is mediated through the Toll-like receptor 4 (TLR4)–myeloid differentiation factor 2 (MD2) complex. Surface plasmon resonance analysis indicated that CIRP binds to the TLR4-MD2 complex, as well as to TLR4 and MD2 individually. In particular, human CIRP amino acid residues 106–125 bind to MD2 with high affinity. Thus, CIRP is a damage-associated molecular pattern molecule that promotes inflammatory responses in shock and sepsis.

Thirty-seven million people are admitted to the emergency room with traumatic injury each year, and these injuries are a leading cause of death in the United States[1]. Hemorrhagic shock from loss of blood volume is a major cause of morbidity and mortality after trauma[2]. During fluid resuscitation, excessive amounts of inflammatory cytokines are produced, causing systemic inflammatory response syndrome and multiple organ dysfunction[3]. Sepsis is also associated with systemic inflammatory response syndrome and is frequently observed in the intensive care unit (ICU), with an overall mortality of 30% in the United States[4]. Sepsis was originally defined as severe systemic inflammation that occurs in a host in response to invading pathogens[5].

Systemic inflammation can be triggered by exogenous pathogen-associated molecular pattern molecules (PAMPs) that are expressed on invading microorganisms during infection or by endogenous damage-associated molecular pattern molecules (DAMPs) that are released from host cells during tissue injury[6,7]. Both PAMPs and endogenous DAMPs are recognized by immune cells through a group of pattern-recognition receptors (PRRs), including TLRs, receptors of advanced glycation end products (RAGEs, also called AGERs), C-type lectin receptors, scavenger receptors and complement receptors[8–10]. After binding the receptors, several signaling pathways are activated, leading to the production of inflammatory mediators such as cytokines, chemokines and vasoactive peptides[6,11,12]. Although the involvement of microbial PAMPs is well supported, an understanding of the role of endogenous molecules in inducing inflammation has just begun to emerge. In recent years, several molecules varying in both structure and intracellular function have been identified as alarmin danger signals in triggering immune responses. Members of this growing alarmin family include HMGB1 (refs. 13,14), heat shock proteins[15], uric acid[16], S100 proteins[17], histones[18] and mitochondrial DNA[19].

CIRP belongs to the family of cold shock proteins that respond to cold stresses. Murine and human CIRP are 172-residue (95% identical) nuclear proteins consisting of one N-terminal consensus-sequence RNA-binding domain and one C-terminal glycine-rich domain, and these proteins function as RNA chaperones to facilitate translation (**Supplementary Fig. 1**)[20–22]. CIRP is constitutively expressed at low levels in various tissues[20,23,24] and is upregulated during mild hypothermia[22], exposure to ultraviolet (UV) irradiation[25] and hypoxia[26]. Here we found that extracellular CIRP is an endogenous proinflammatory mediator and DAMP that triggers inflammatory responses during hemorrhagic shock and sepsis.

RESULTS

CIRP levels are increased in hemorrhaged humans and animals

To explore the role of CIRP in clinical conditions, we examined expression of CIRP in sera from ten individuals admitted to the surgical ICU (**Supplementary Table 1**; five females and five males with an average age of 71 years). The Acute Physiology and Chronic

[1]Center for Translational Research, The Feinstein Institute for Medical Research, Manhasset, New York, USA. [2]Center for Biomedical Science, The Feinstein Institute for Medical Research, Manhasset, New York, USA. [3]Department of Clinical Molecular Biology, Kyoto University, Kyoto, Japan. [4]These authors contributed equally to this work. Correspondence should be addressed to P.W. (pwang@nshs.edu).

Received 2 April; accepted 6 September; published online 6 October 2013; doi:10.1038/nm.3368

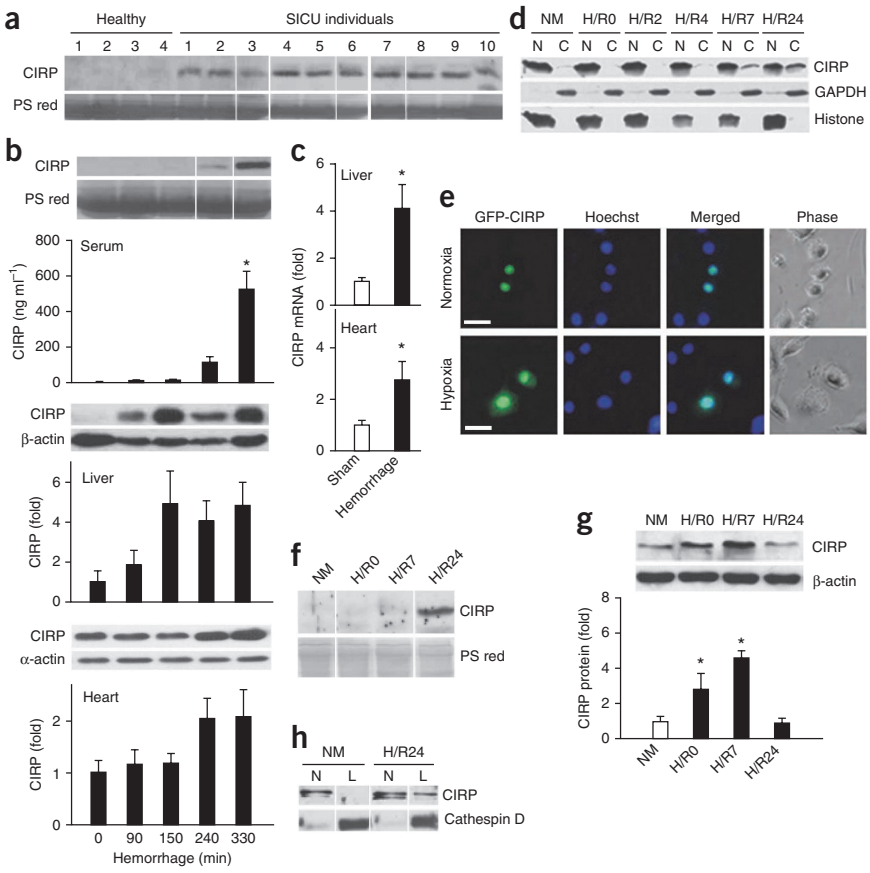

Figure 1 Increased expression and release of CIRP after hemorrhage. (**a**) Western blot analysis of CIRP in the serum of healthy volunteers and individuals admitted to the surgical ICU (SICU) with shock. PS red, Ponceau S red staining. (**b**) Western blot analysis of CIRP in the tissues of rats at the indicated times after hemorrhage. $n = 4$–6 rats per time-point. $^*P < 0.05$ compared to time 0 determined by one-way analysis of variance (ANOVA) and Student-Newman-Keuls test. (**c**) Quantitative PCR analysis of CIRP mRNA in the liver and heart of rats at 240 min after hemorrhage. $n = 6$ rats per group. $^*P < 0.05$ compared to sham determined by Student's t test. (**d**) Western blot analysis of CIRP in the nuclear (N) and cytoplasmic (C) compartments of RAW 264.7 cells cultured under normoxic (NM) or hypoxic (1% O_2) conditions for 20 h followed by reoxygenation for 0, 2, 4, 7 or 24 h (H/R0, H/R2, H/R4, H/R7 or H/R24, respectively). Antibodies to glyceraldehyde 3-phosphate dehydrogenase (GAPDH) and histone were used to detect the cytoplasm and nucleus, respectively. (**e**) Images of RAW 264.7 cells expressing GFP-CIRP (green) and Hoechst 33245 (blue) staining of nuclei. Scale bars, 25 μm. (**f**,**g**) Western blot analysis of CIRP in conditioned medium (**f**) or total cell lysates (**g**) from RAW 264.7 cells. $n = 3$ independent experiments. $^*P < 0.05$ compared to NM determined by one-way ANOVA and Student-Newman-Keuls test. (**h**) Western blot analysis of CIRP in the nuclear and lysosomal (L) components of RAW 264.7 cells cultured in normoxia or exposed to hypoxia/reperfusion for 24 h (H/R24). Antibody to cathepsin D was used to detect lysosomes. The images in **d**–**h** represent three independent experiments. The data in **b**, **c** and **g** are shown as the mean ± s.e.m. For the western blot images, the small gaps indicate skipped lanes from the same membrane, and large gaps indicate separate membranes.

Health Evaluation II (APACHE II) scores for these individuals ranged from 13 to 25, with an average of 19. The average blood sample collection time was 43 h after the onset of shock, which was defined by a clinically documented systolic blood pressure <90 mm Hg either during active hemorrhage or after a traumatic insult. Serum CIRP was readily detectable in all ten individuals regardless of differences in clinical parameters, whereas serum CIRP was barely detectable in healthy volunteers (**Fig. 1a**).

We induced hemorrhagic shock in rats by bleeding animals to a mean arterial pressure of 25–30 mm Hg and maintaining that pressure for 90 min. We then provided fluid resuscitation. Serum CIRP was detectable at 240 min, and serum CIRP levels were significantly elevated at 330 min post shock in hemorrhaged rats (**Fig. 1b**). CIRP protein levels were nonsignificantly increased at 150 and 240 min in the liver and heart, respectively (**Fig. 1b**). CIRP mRNA levels were significantly induced by 4.1-fold and 2.8-fold in the liver and heart, respectively, at 240 min post shock (**Fig. 1c**).

CIRP is released from macrophages exposed to hypoxia

Because CIRP was detectable in the serum of both humans and rats after shock, we attempted to determine the mode of CIRP release. Macrophages are a major cell population responsible for the release of inflammatory mediators after injury. We cultured mouse macrophage-like RAW 264.7 cells under hypoxic conditions to mimic conditions occurring during hemorrhagic shock and examined the cellular location of CIRP. CIRP was located primarily in the nucleus during normoxic conditions (**Fig. 1d**). When we subjected cells to 20 h of hypoxia, CIRP expression was detectable in the cytoplasm at 7 h after reoxygenation and was markedly increased at 24 h after reoxygenation, as determined by biochemical fractionation (**Fig. 1d**). By using a molecular biology approach, we observed that GFP-CIRP expression (green fluorescence) in the nucleus overlapped with Hoechst staining in RAW 264.7 cells under normoxia (**Fig. 1e**), whereas GFP alone was expressed throughout the cell (**Supplementary Fig. 2**). However, when we subjected cells to hypoxia, we observed GFP-CIRP expression in the nucleus and cytoplasm at 4 h after reoxygenation (**Fig. 1e**).

We then examined release of cytoplasmic CIRP into the extracellular space. In the conditioned medium of RAW 264.7 cells, CIRP was undetectable in normoxia but was released at 24 h after reoxygenation, as determined by western blotting (**Fig. 1f**). Furthermore, intracellular CIRP protein levels increased by 2.8-fold as compared to normoxia immediately after hypoxia and by 4.3-fold after 7 h of reoxygenation but were then reduced after 24 h of reoxygenation, potentially because of the release of CIRP into the medium (**Fig. 1f**,**g**). CIRP release was not attributable to necrosis, as there was no change in lactate dehydrogenase activity and no detectable intracellular BCL2-associated X protein (BAX) in the conditioned medium after hypoxia (data not shown).

The CIRP protein sequence does not contain a secretion leader signal, suggesting that its secretion should not be mediated through

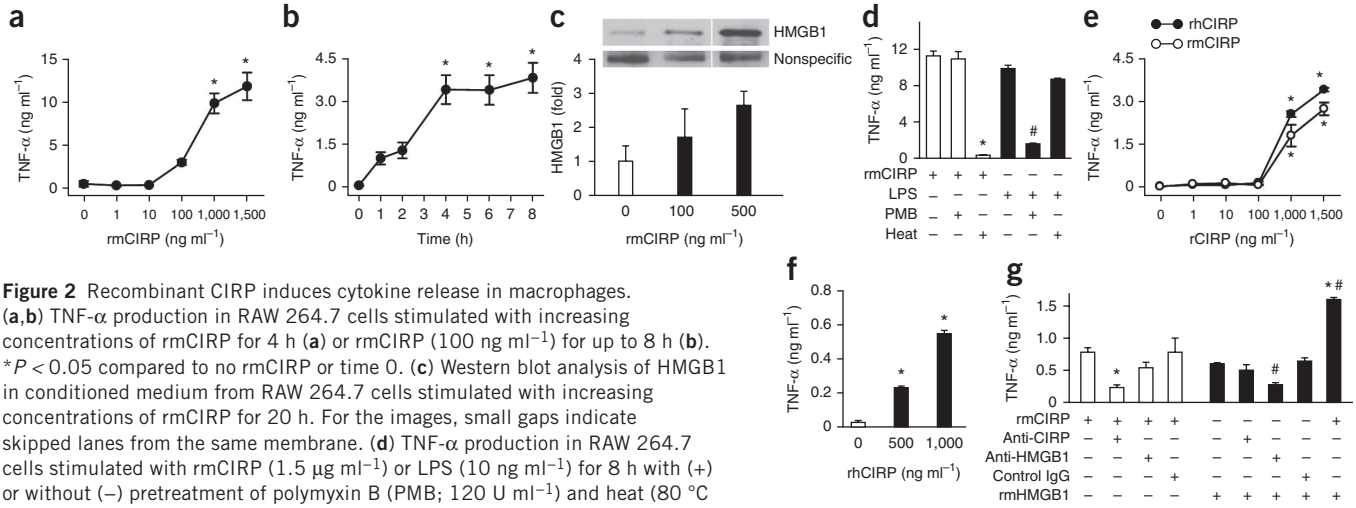

Figure 2 Recombinant CIRP induces cytokine release in macrophages. (**a**,**b**) TNF-α production in RAW 264.7 cells stimulated with increasing concentrations of rmCIRP for 4 h (**a**) or rmCIRP (100 ng ml^{-1}) for up to 8 h (**b**). $^{*}P < 0.05$ compared to no rmCIRP or time 0. (**c**) Western blot analysis of HMGB1 in conditioned medium from RAW 264.7 cells stimulated with increasing concentrations of rmCIRP for 20 h. For the images, small gaps indicate skipped lanes from the same membrane. (**d**) TNF-α production in RAW 264.7 cells stimulated with rmCIRP (1.5 μg ml^{-1}) or LPS (10 ng ml^{-1}) for 8 h with (+) or without (–) pretreatment of polymyxin B (PMB; 120 U ml^{-1}) and heat (80 °C for 30 min). $^{*}P < 0.05$ compared to rmCIRP, $^{\#}P < 0.05$ compared to LPS. (**e**) TNF-α production in differentiated human THP-1 cells stimulated with increasing concentrations of rhCIRP or rmCIRP for 4 h. $^{*}P < 0.05$ compared to no CIRP. (**f**) TNF-α production in human PBMCs stimulated with increasing concentrations of rhCIRP for 8 h. $^{*}P < 0.05$ compared to no rhCIRP. (**g**) TNF-α production in THP-1 cells stimulated with rmCIRP (0.3 μg ml^{-1}), rmHMGB1 (0.3 μg ml^{-1}) or rmCIRP plus rmHMGB1 for 8 h with (+) or without (–) 1 h of preincubation with antisera to CIRP (anti-CIRP; 4 μg ml^{-1}), antisera to HMGB1 (anti-HMGB1; 4 μg ml^{-1}) or rabbit control (nonimmunized) IgG (4 μg ml^{-1}). $^{*}P < 0.05$ compared to rmCIRP, $^{\#}P < 0.05$ compared to rmHMGB1. All data throughout the figure are shown as the mean ± s.e.m. $n = 3$ independent experiments in all panels except for **g**, in which $n = 4$. All statistical significance was determined by one-way ANOVA and Student-Newman-Keuls test.

the classical (endoplasmic reticulum–Golgi dependent) pathway[27]. To identify a potential mechanism of active CIRP release, we conducted biochemical fractionation to isolate the lysosomal compartment of RAW 264.7 cells undergoing hypoxia. During normoxia, CIRP protein was not detectable in lysosomes, but it colocalized with cathepsin D, a protein maker of lysosomes, at 24 h after reoxygenation from hypoxia (**Fig. 1h**), suggesting that CIRP may be released by lysosomal secretion.

Recombinant CIRP induces inflammatory responses

To address whether extracellular CIRP could function as an inflammatory mediator, we expressed and purified recombinant murine CIRP (rmCIRP) using a bacterial expression system with more than 97% purity (**Supplementary Fig. 3a**,**b**). We conducted a Triton X-114 extraction procedure to remove lipopolysaccharide (LPS)[28] from the purified rmCIRP. We detected a residual ~10 pg of LPS per μg of CIRP by the Limulus amebocyte lysate assay, which was comparable to that described in other identified endogenous DAMPs expressed and purified from bacteria[29,30]. rmCIRP increased TNF-α release from cultured RAW 264.7 cells in a dose- and time-dependent manner (**Fig. 2a**,**b**). rmCIRP also dose-dependently induced the release of another proinflammatory cytokine, HMGB1 (**Fig. 2c**). *In vivo*, administration of rmCIRP to healthy rats increased serum TNF-α, interleukin-6 (IL-6) and HMGB1 levels and induced liver injury, as assessed by increased levels of the organ injury markers aspartate aminotransferase (AST) and alanine aminotransferase (ALT) (**Supplementary Fig. 4**).

To rule out a contribution from LPS in the inflammatory response to rmCIRP, we found that incubation with polymyxin B, an LPS-binding antibiotic, did not interfere with rmCIRP-induced production of TNF-α, whereas heat treatment reduced the activity of rmCIRP (**Fig. 2d**). In contrast, polymyxin B inhibited LPS-induced TNF-α release by 84%, whereas heat treatment on LPS only slightly attenuated the amount of TNF-α released in response to LPS (**Fig. 2d**). To further avoid LPS contamination in the preparation of recombinant proteins, we obtained the expressed and purified recombinant human CIRP (rhCIRP) from human HEK293 cells. rhCIRP had comparable activity to rmCIRP in dose-dependently stimulating TNF-α release from differentiated human THP-1 cells (**Fig. 2e**) and primary human peripheral blood mononuclear cells (PBMCs) (**Fig. 2f**). Thus, CIRP-induced cytokine activation is conserved between rodents and humans and is not due to LPS contamination.

HMGB1 can also stimulate TNF-α release[31]. We analyzed the relationship between CIRP and HMGB1 in stimulating TNF-α release by applying neutralizing antisera to each. We generated antisera to CIRP that effectively inhibited rmCIRP-induced TNF-α production in RAW 264.7 cells (**Supplementary Fig. 3c**,**d**). Preincubation of THP-1 cells with antisera to HMGB1 (ref. 32) reduced rmCIRP-induced TNF-α release nonsignificantly by 31%, whereas preincubation with antisera to CIRP resulted in a 70% reduction (**Fig. 2g**). Conversely, preincubation of THP-1 cells with antisera to CIRP resulted in only a 17% (nonsignificant) reduction of TNF-α release induced by rmHMGB1 (**Fig. 2g**). In addition, rmCIRP, rmHMGB1 and rmCIRP plus rmHMGB1 induced TNF-α levels of 0.8, 0.6 and 1.6 ng ml^{-1}, respectively (**Fig. 2g**). Taken together, these results indicate that CIRP and HMGB1 additively stimulate TNF-α release from macrophages.

Neutralization of CIRP attenuates hemorrhage and sepsis

We next determined whether extracellular CIRP has a role in mediating inflammatory responses during hemorrhage. Administration of neutralizing antisera to CIRP during fluid resuscitation to hemorrhaged rats significantly reduced serum and hepatic levels of TNF-α and IL-6 as compared to hemorrhaged rats given control IgG (**Fig. 3a**). Serum AST and ALT, as well as liver myeloperoxidase activity, which is indicative of neutrophil accumulation, were significantly reduced in the group administered the antisera to CIRP (**Fig. 3b**). The survival rate in the rats administered the antisera to CIRP was significantly higher than that in the groups administered control IgG or vehicle at

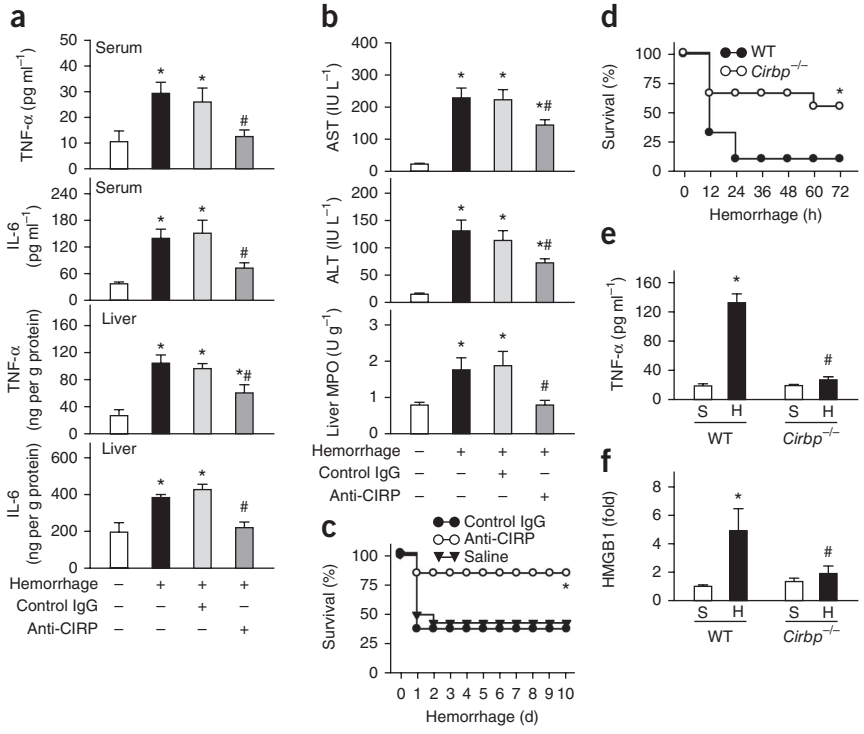

Figure 3 Blockade of CIRP reduces TNF-α and IL-6 production, hepatic injury and mortality after hemorrhage. (**a**,**b**) TNF-α and IL-6 levels in the serum and liver, as well as the activity of the hepatic injury markers AST, ALT and liver myeloperoxidase (MPO), in rats at 4 h after hemorrhage. Hemorrhaged rats received rabbit control (nonimmunized) IgG or antisera to CIRP (10 mg per kg body weight) during fluid resuscitation. $n = 6$ rats per group. $^{*}P < 0.05$ compared to sham, $^{\#}P < 0.05$ compared to hemorrhage alone. (**c**) Survival curves of hemorrhaged rats administered normal saline ($n = 14$), control IgG (10 mg per kg body weight, $n = 13$) or antisera to CIRP (10 mg per kg body weight, $n = 13$) for 3 consecutive days. $^{*}P < 0.05$ compared to saline. (**d**) Survival curves of hemorrhaged wild-type (WT) and *Cirbp*$^{-/-}$ mice. $n = 9$ mice per group. $^{*}P < 0.05$ compared to WT. (**e**,**f**) Serum TNF-α (**e**) and HMGB1 (**f**) levels in WT and *Cirbp*$^{-/-}$ mice at 4 h after hemorrhage. $n = 6$ mice per group, $^{*}P < 0.05$ compared to WT sham, $^{\#}P < 0.05$ compared to WT hemorrhage. All data throughout the figure are shown as the mean ± s.e.m. Statistical significance was determined by one-way ANOVA and Student-Newman-Keuls test (**a**,**b**,**e**,**f**) or log-rank test (**c**,**d**).

10 d after hemorrhage (85% compared to 38% and 43%, respectively; **Fig. 3c**). In concordance with antisera-mediated blockade of CIRP, the survival rate of *Cirbp*$^{-/-}$ mice was significantly higher than that of wild-type mice at 72 h after hemorrhage (56% compared to 11%, respectively; **Fig. 3d**). We also observed a notable increase in serum TNF-α (**Fig. 3e**) and HMGB1 (**Fig. 3f**) levels in wild-type mice at 4 h after hemorrhage, which was considerably reduced in *Cirbp*$^{-/-}$ mice (**Fig. 3e**). These findings suggest that CIRP and HMGB1 both contribute to inflammation and mortality after shock.

We then extended the study of the proinflammatory activity of CIRP to sepsis. We examined CIRP expression in rats subjected to cecal ligation and puncture (CLP), an established animal model of polymicrobial sepsis[33]. At 20 h after CLP, serum levels of CIRP were increased by 3.4-fold as compared to sham-operated controls (**Fig. 4a**). Similarly, mRNA and protein levels of CIRP in the liver were also increased by 2.4-fold and 4.0-fold, respectively, at 20 h after CLP (**Fig. 4b**,**c**). We also assessed the effect of LPS on CIRP expression and release *in vitro*. The mRNA and protein expression of CIRP in isolated rat primary peritoneal macrophages were increased after exposure to LPS for 6 and 24 h, respectively (**Fig. 4d**,**e**). CIRP protein was also detectable in the conditioned medium after 6 h of exposure to LPS (**Fig. 4e**). We then examined whether other inflammatory mediators induce CIRP release. Incubation of RAW 264.7 cells with rmHMGB1 and rmTNF-α for 24 h did not induce CIRP release into the medium, whereas CIRP protein was detectable in the medium from cells exposed to LPS (**Fig. 4f**). To assess whether extracellular

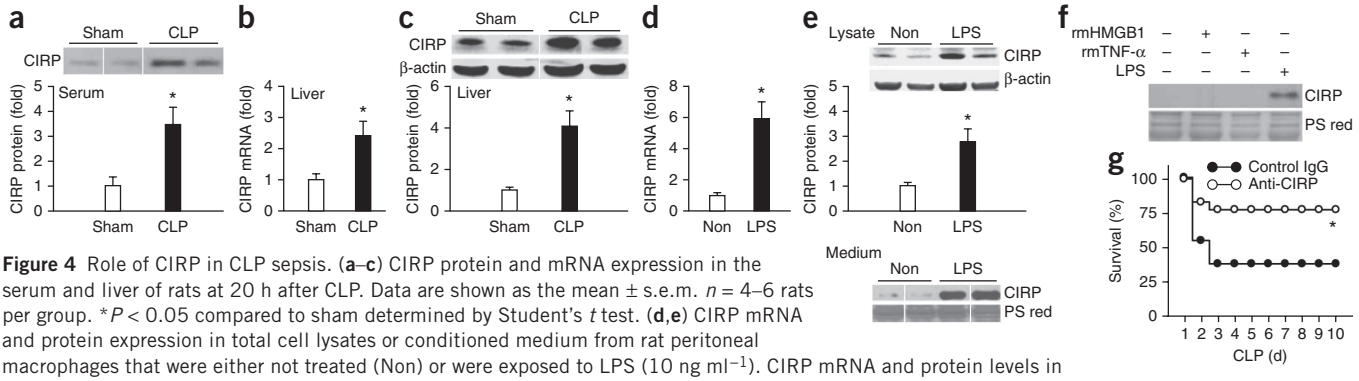

Figure 4 Role of CIRP in CLP sepsis. (**a**–**c**) CIRP protein and mRNA expression in the serum and liver of rats at 20 h after CLP. Data are shown as the mean ± s.e.m. $n = 4$–6 rats per group. $^{*}P < 0.05$ compared to sham determined by Student's *t* test. (**d**,**e**) CIRP mRNA and protein expression in total cell lysates or conditioned medium from rat peritoneal macrophages that were either not treated (Non) or were exposed to LPS (10 ng ml^{-1}). CIRP mRNA and protein levels in the conditioned medium were determined after 6 h of LPS exposure. CIRP protein in total cell lysates was determined after 24 h of LPS exposure. Data are shown as the mean ± s.e.m. $n = 3$ independent experiments. $^{*}P < 0.05$ compared to the untreated group determined by Student's *t* test. (**f**) Western blot analysis of CIRP in the conditioned medium of RAW 264.7 cells stimulated with (+) or without (–) rmHMGB1 (1 μg ml^{-1}), rmTNF-α (30 ng ml^{-1}) and LPS (100 ng ml^{-1}) for 24 h. The images represent three independent experiments. (**g**) Survival curves of rats after induction of polymicrobial sepsis that were administered rabbit control (nonimmunized) IgG (10 mg per kg body weight) or antisera to CIRP 5 h after CLP (10 mg per kg body weight). $n = 18$ rats per group. $^{*}P < 0.05$ compared to control IgG determined by log-rank test. For the western blot images, small gaps indicate skipped lanes from the same membrane.

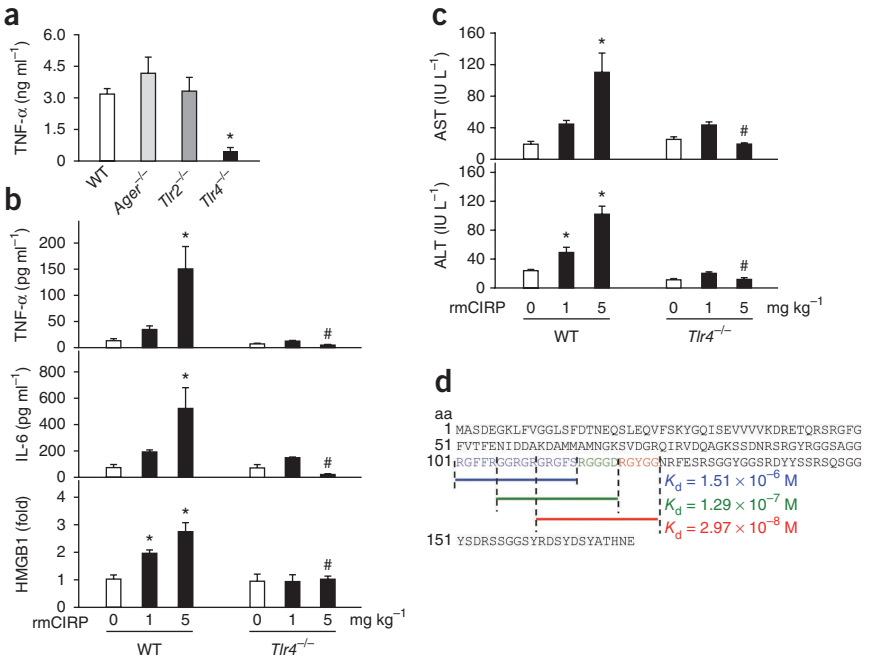

Figure 5 The TLR4-MD2 complex mediates extracellular CIRP activity. (**a**) TNF-α production in peritoneal macrophages from WT, *Ager*$^{-/-}$, *Tlr2*$^{-/-}$ and *Tlr4*$^{-/-}$ mice stimulated with rmCIRP (1.5 μg ml^{-1}) for 4 h. Data are shown as the mean ± s.e.m. $n = 3$ independent experiments. $^{*}P < 0.05$ compared to WT. (**b**,**c**) Serum levels of TNF-α, IL-6, HMGB1, AST and ALT in WT and *Tlr4*$^{-/-}$ mice at 4 h after administration of normal saline (rmCIRP 0) or rmCIRP (1 or 5 mg per kg body weight). Data are shown as the mean ± s.e.m. $n = 6$–9 mice per group. $^{*}P < 0.05$ compared to WT and no rmCIRP, $^{\#}P < 0.05$ compared to WT with rmCIRP (5 mg per kg body weight). (**d**) Binding affinities (K_d) of three oligopeptides derived from the human CIRP sequence to rhMD2. aa, amino acid. Representative sensorgrams of the oligopeptide analysis from two independent experiments are shown in **Supplementary Figure 6**. All statistical significance was determined by one-way ANOVA and Student-Newman-Keuls test.

CIRP contributes to mortality in sepsis, we administered neutralizing antisera to CIRP to septic animals 5 h after CLP. The 10-d survival rate of septic rats significantly increased from 39% to 78% in rats treated with antisera to CIRP (**Fig. 4g**). Thus, CIRP also contributes to mortality in sepsis.

CIRP induces inflammatory responses through TLR4

We then determined which cell surface receptors are bound by extracellular CIRP. We examined three major PRRs that are known to mediate inflammatory responses: RAGE (also called AGER), TLR2 and TLR4 (refs. 8–10). By comparing the differences in response to rmCIRP between macrophages from wild-type mice and mice deficient in each receptor, we found that only TLR4-deficient macrophages lost the response to rmCIRP (in terms of TNF-α induction), whereas RAGE- and TLR2-deficient macrophages maintained similar responses as wild-type macrophages (**Fig. 5a**). To confirm the requirement of TLR4 in mediating CIRP activity, we injected rmCIRP into wild-type and *Tlr4*$^{-/-}$ mice. Similar to rats, wild-type mice exhibited an increase in the levels of serum proinflammatory cytokines (TNF-α, IL-6 and HMGB1) and organ injury markers (AST and ALT) in a dose-dependent manner in response to rmCIRP injection (**Fig. 5b**,**c**), which were diminished in *Tlr4*$^{-/-}$ mice (**Fig. 5b**,**c**).

We then performed surface plasmon resonance (SPR) analysis to validate the physical interaction between CIRP and the receptors. TLR4 often binds to MD2 as a co-receptor to form the TLR4-MD2 complex[34]. We used the recombinant proteins derived from the human coding sequence for SPR analysis. rhCIRP bound to rhTLR4, rhMD2 and the rhTLR4-MD2 complex with apparent dissociation constants (K_d) of 6.17 × 10^{-7}, 3.02 × 10^{-7} and 2.39 × 10^{-7} M, respectively (**Table 1** and **Supplementary Fig. 5**). We also examined the binding of rhMD2 to rhTLR4 as a positive control and obtained an apparent K_d of 5.37 × 10^{-8} M, which is similar to the K_d of 6.29 × 10^{-8} M that was reported in a recent study[35]. Notably, rhCIRP had a K_d in the nanomolar range in terms of binding to RAGE and TLR2 (**Table 1** and **Supplementary Fig. 5**); however, the biological importance of this remains to be determined. To determine the region of CIRP that bound to MD2, we synthesized 32 oligopeptides (15-mer) covering the entire human CIRP sequence and performed a series of SPR analyses. Three oligopeptides, residues 101–115, 106–120 and 111–125, bound to rhMD2 with high affinity (**Fig. 5d** and **Supplementary Fig. 6**).

DISCUSSION

Intracellular CIRP is currently thought to stabilize specific mRNAs and facilitate translation for a survival advantage when cells are under stress[36,37]. In this study, we provide several lines of evidence that extracellular CIRP is also a DAMP.

We demonstrated that CIRP translocates from the nucleus to the cytoplasm after exposure to hypoxia. Translocation of CIRP has also been observed in other cell types, including fibroblasts and epithelial cells, after exposure to UV irradiation, osmotic shock, heat shock or endoplasmic reticulum stresses[38,39]. Methylation of arginine residues in the RGG domain of CIRP after environmental stress[38] and phosphorylation in the C-terminal region in response to UV irradiation[39] have been postulated to regulate the exit of CIRP from the nucleus. We also observed the release of CIRP into conditioned medium in response to hypoxia or LPS. A number of noncanonical pathways have been proposed for the release of 'leaderless' proteins, including microvesicle shedding, exocytosis of secretory lysosomes and active transport[27]. In addition, an alternative model of leaderless IL-1β secretion has been proposed that involves the formation of multivesicular bodies containing exosomes with entrapped IL-1β and fusion of these multivesicular bodies with the plasma membrane to release

Table 1 Binding affinities of rhCIRP to pattern recognition receptors and MD2

Analyte	Immobilized	K_d (M)
rhCIRP	rhTLR4	6.17 × 10^{-7}
rhMD2	rhCIRP	3.02 × 10^{-7}
rhTLR4-MD2	rhCIRP	2.39 × 10^{-7}
rhMD2	rhTLR4	5.37 × 10^{-8}
rhRAGE	rhCIRP	3.31 × 10^{-8}
rhTLR2	rhCIRP	2.58 × 10^{-7}

Representative sensorgrams of analyte interactions are shown in **Supplementary Figure 5** from two to three independent experiments.

the exosomes[40]. Although we demonstrated that CIRP can be released through the lysosomal secretion, other mechanisms responsible for CIRP release require further investigation.

Identification of the TLR4–mediated proinflammatory activity of CIRP is consistent with previous studies showing that TLR4 has a major role in mediating inflammation and organ injury in hemorrhaged[41] and septic animals[42]. TLR4 can also recognize several endogenous molecules, including HMGB1, heat shock proteins, hyaluronic acid and fibronectin, when they are released from stressed, damaged or dying cells or from degradation of the extracellular matrix[43–46]. Although many DAMPs serve as ligands of the TLR4-MD2 complex, some molecules may bind to the different sites of the TLR4-MD2 complex and work additively in stimulating proinflammatory cytokine production in macrophages, as we have demonstrated here through the relationship between CIRP and HMGB1. As indicated by SPR analysis, HMGB1 binds to the TLR4-MD2 complex with a K_d of 1.5×10^{-6} M[47], which is comparable to that of CIRP ($K_d = 2.39 \times 10^{-7}$ M). HMGB1 has been shown to bind to MD2 with a K_d of 8×10^{-9} M but to not bind to TLR4 (ref. 48), whereas we found here that CIRP can bind to both MD2 and TLR4 individually. Additional mapping of the subdomains of CIRP that interact with TLR4, MD2 and the TLR4-MD2 complex will help ascertain how CIRP binds to and activates these receptors. Of note, the K_d values of LPS to TLR4 and MD2 are 1.41×10^{-5} and 2.33×10^{-6} M, respectively[49]. In addition to the binding of the TLR4-MD2 complex, we also observed that CIRP can bind to TLR2 and RAGE, which fits its character as a chaperone protein to interact with different types of proteins.

Discovery of CIRP as an inflammatory mediator and DAMP not only advances our understanding of additional proinflammatory mediators but will also help in the development of new therapeutic strategies. We demonstrated that CIRP can be actively released, despite the fact that leaderless proteins can be leaked out by passive modes, such as necrosis[50]. In support of our findings, a recent study reported the involvement of CIRP in activating the nuclear factor-κB (NF-κB) pathway and regulating IL-1β expression in cultured fibroblasts[51]. As neutralizing antisera to CIRP attenuate inflammatory responses and improve the survival of hemorrhaged and septic animals, CIRP may be targeted therapeutically to reduce morbidity and mortality in individuals with hemorrhage and sepsis.

METHODS

Methods and any associated references are available in the online version of the paper.

Note: Any Supplementary Information and Source Data files are available in the online version of the paper.

ACKNOWLEDGMENTS

This work was supported by US National Institutes of Health (NIH) grants HL076179 and GM053008 (P.W.). We thank H. Erlandsson-Harris (Karolinska Institute) for providing *Ager*$^{-/-}$, *Tlr2*$^{-/-}$ and *Tlr4*$^{-/-}$ mice, M. Hu, J.H. Li and L.M. Corbo for technical assistance, L. Caracappa for editorial assistance and Y. Al-Abed and A. Ragab for assistance with SPR analysis. The BIAcore instrument was supported by NIH grant S10OD012042. J.F. was partly supported by the Smoking Research Foundation of Japan.

AUTHOR CONTRIBUTIONS

X.Q. and M.Z. performed the experiments and analyzed data. W.-L.Y. conducted the translocation study, designed and coordinated SPR analysis and wrote the manuscript. R.W. designed the experiments. A.J. assisted with the design of experiments and participated in manuscript editing. W.D. and Y.J. performed animal studies. M.K. collected the serum from patients admitted to the surgical ICU and analyzed human data. J.N. and G.F.C. analyzed animal studies. H.Y. and K.J.T. assisted in the knockout mice study and SPR analysis. J.F. assisted in the CIRP knockout mice and GFP-CIRP study and revised the manuscript. H.W. assisted with the design of the study and analyzed data. P.W. designed and supervised the study and revised the manuscript.

COMPETING FINANCIAL INTERESTS

The authors declare competing financial interests: details are available in the online version of the paper.

1. Holcomb, J.B. *et al.* Challenges to effective research in acute trauma resuscitation: consent and endpoints. *Shock* **35**, 107–113 (2011).
2. Bulger, E.M. *et al.* Hypertonic resuscitation of hypovolemic shock after blunt trauma: a randomized controlled trial. *Arch. Surg.* **143**, 139–148 (2008).
3. Kaczorowski, D.J., Mollen, K.P., Edmonds, R. & Billiar, T.R. Early events in the recognition of danger signals after tissue injury. *J. Leukoc. Biol.* **83**, 546–552 (2008).
4. Dombrovskiy, V.Y., Martin, A.A., Sunderram, J. & Paz, H.L. Rapid increase in hospitalization and mortality rates for severe sepsis in the United States: a trend analysis from 1993 to 2003. *Crit. Care Med.* **35**, 1244–1250 (2007).
5. Ward, P.A. New approaches to the study of sepsis. *EMBO Mol. Med.* **4**, 1234–1243 (2012).
6. Medzhitov, R. Origin and physiological roles of inflammation. *Nature* **454**, 428–435 (2008).
7. Oppenheim, J.J. & Yang, D. Alarmins: chemotactic activators of immune responses. *Curr. Opin. Immunol.* **17**, 359–365 (2005).
8. Zhang, X. & Mosser, D.M. Macrophage activation by endogenous danger signals. *J. Pathol.* **214**, 161–178 (2008).
9. Beutler, B.A. TLRs and innate immunity. *Blood* **113**, 1399–1407 (2009).
10. Ward, P.A. The sepsis seesaw: seeking a heart salve. *Nat. Med.* **15**, 497–498 (2009).
11. Kawai, T. & Akira, S. The role of pattern-recognition receptors in innate immunity: update on Toll-like receptors. *Nat. Immunol.* **11**, 373–384 (2010).
12. Chen, G.Y., Tang, J., Zheng, P. & Liu, Y. CD24 and Siglec-10 selectively repress tissue damage–induced immune responses. *Science* **323**, 1722–1725 (2009).
13. Wang, H. *et al.* HMG-1 as a late mediator of endotoxin lethality in mice. *Science* **285**, 248–251 (1999).
14. Tsung, A. *et al.* The nuclear factor HMGB1 mediates hepatic injury after murine liver ischemia-reperfusion. *J. Exp. Med.* **201**, 1135–1143 (2005).
15. Quintana, F.J. & Cohen, I.R. Heat shock proteins as endogenous adjuvants in sterile and septic inflammation. *J. Immunol.* **175**, 2777–2782 (2005).
16. Martinon, F., Pétrilli, V., Mayor, A., Tardivel, A. & Tschopp, J. Gout-associated uric acid crystals activate the NALP3 inflammasome. *Nature* **440**, 237–241 (2006).
17. Vogl, T. *et al.* Mrp8 and Mrp14 are endogenous activators of Toll-like receptor 4, promoting lethal, endotoxin-induced shock. *Nat. Med.* **13**, 1042–1049 (2007).
18. Xu, J. *et al.* Extracellular histones are major mediators of death in sepsis. *Nat. Med.* **15**, 1318–1321 (2009).
19. Zhang, Q. *et al.* Circulating mitochondrial DAMPs cause inflammatory responses to injury. *Nature* **464**, 104–107 (2010).
20. Nishiyama, H. *et al.* Cloning and characterization of human CIRP (cold-inducible RNA-binding protein) cDNA and chromosomal assignment of the gene. *Gene* **204**, 115–120 (1997).
21. Nishiyama, H. *et al.* A glycine-rich RNA-binding protein mediating cold-inducible suppression of mammalian cell growth. *J. Cell Biol.* **137**, 899–908 (1997).
22. Xue, J.H. *et al.* Effects of ischemia and H_2O_2 on the cold stress protein CIRP expression in rat neuronal cells. *Free Radic. Biol. Med.* **27**, 1238–1244 (1999).
23. Nishiyama, H. *et al.* Decreased expression of cold-inducible RNA-binding protein (CIRP) in male germ cells at elevated temperature. *Am. J. Pathol.* **152**, 289–296 (1998).
24. Nishiyama, H. *et al.* Diurnal change of the cold-inducible RNA-binding protein (Cirp) expression in mouse brain. *Biochem. Biophys. Res. Commun.* **245**, 534–538 (1998).
25. Sheikh, M.S. *et al.* Identification of several human homologs of hamster DNA damage–inducible transcripts. Cloning and characterization of a novel UV-inducible cDNA that codes for a putative RNA-binding protein. *J. Biol. Chem.* **272**, 26720–26726 (1997).
26. Wellmann, S. *et al.* Oxygen-regulated expression of the RNA-binding proteins RBM3 and CIRP by a HIF-1–independent mechanism. *J. Cell Sci.* **117**, 1785–1794 (2004).
27. Qu, Y. & Dubyak, G.R. P2X7 receptors regulate multiple types of membrane trafficking responses and non-classical secretion pathways. *Purinergic Signal.* **5**, 163–173 (2009).
28. Aida, Y. & Pabst, M.J. Removal of endotoxin from protein solutions by phase separation using Triton X-114. *J. Immunol. Methods* **132**, 191–195 (1990).
29. Wang, Y. *et al.* Identification of stimulating and inhibitory epitopes within the heat shock protein 70 molecule that modulate cytokine production and maturation of dendritic cells. *J. Immunol.* **174**, 3306–3316 (2005).

30. Henderson, B. *et al.* Caught with their PAMPs down? The extracellular signalling actions of molecular chaperones are not due to microbial contaminants. *Cell Stress Chaperones* **15**, 123–141 (2010).
31. Andersson, U. *et al.* High mobility group 1 protein (HMG-1) stimulates proinflammatory cytokine synthesis in human monocytes. *J. Exp. Med.* **192**, 565–570 (2000).
32. Yang, H. *et al.* Reversing established sepsis with antagonists of endogenous high-mobility group box 1. *Proc. Natl. Acad. Sci. USA* **101**, 296–301 (2004).
33. Yang, S., Zhou, M., Chaudry, I.H. & Wang, P. Novel approach to prevent the transition from the hyperdynamic phase to the hypodynamic phase of sepsis: role of adrenomedullin and adrenomedullin binding protein-1. *Ann. Surg.* **236**, 625–633 (2002).
34. Nagai, Y. *et al.* Essential role of MD-2 in LPS responsiveness and TLR4 distribution. *Nat. Immunol.* **3**, 667–672 (2002).
35. Hyakushima, N. *et al.* Interaction of soluble form of recombinant extracellular TLR4 domain with MD-2 enables lipopolysaccharide binding and attenuates TLR4-mediated signaling. *J. Immunol.* **173**, 6949–6954 (2004).
36. Yang, C. & Carrier, F. The UV-inducible RNA-binding protein A18 (A18 hnRNP) plays a protective role in the genotoxic stress response. *J. Biol. Chem.* **276**, 47277–47284 (2001).
37. Cammas, A., Lewis, S.M., Vagner, S. & Holcik, M. Post-transcriptional control of gene expression through subcellular relocalization of mRNA binding proteins. *Biochem. Pharmacol.* **76**, 1395–1403 (2008).
38. De Leeuw, F. *et al.* The cold-inducible RNA-binding protein migrates from the nucleus to cytoplasmic stress granules by a methylation-dependent mechanism and acts as a translational repressor. *Exp. Cell Res.* **313**, 4130–4144 (2007).
39. Yang, R. *et al.* Functional significance for a heterogenous ribonucleoprotein A18 signature RNA motif in the 3′-untranslated region of ataxia telangiectasia mutated and Rad3-related (ATR) transcript. *J. Biol. Chem.* **285**, 8887–8893 (2010).
40. Qu, Y., Franchi, L., Nunez, G. & Dubyak, G.R. Nonclassical IL-1β secretion stimulated by P2X7 receptors is dependent on inflammasome activation and correlated with exosome release in murine macrophages. *J. Immunol.* **179**, 1913–1925 (2007).
41. Benhamou, Y. *et al.* Toll-like receptors 4 contribute to endothelial injury and inflammation in hemorrhagic shock in mice. *Crit. Care Med.* **37**, 1724–1728 (2009).
42. Wittebole, X., Castanares-Zapatero, D. & Laterre, P.F. Toll-like receptor 4 modulation as a strategy to treat sepsis. *Mediators Inflamm.* **2010**, 568396 (2010).
43. Park, J.S. *et al.* Involvement of toll-like receptors 2 and 4 in cellular activation by high mobility group box 1 protein. *J. Biol. Chem.* **279**, 7370–7377 (2004).
44. Ohashi, K., Burkart, V., Flohé, S. & Kolb, H. Cutting edge: heat shock protein 60 is a putative endogenous ligand of the toll-like receptor-4 complex. *J. Immunol.* **164**, 558–561 (2000).
45. Termeer, C. *et al.* Oligosaccharides of Hyaluronan activate dendritic cells via toll-like receptor 4. *J. Exp. Med.* **195**, 99–111 (2002).
46. Okamura, Y. *et al.* The extra domain A of fibronectin activates Toll-like receptor 4. *J. Biol. Chem.* **276**, 10229–10233 (2001).
47. Yang, H. *et al.* A critical cysteine is required for HMGB1 binding to Toll-like receptor 4 and activation of macrophage cytokine release. *Proc. Natl. Acad. Sci. USA* **107**, 11942–11947 (2010).
48. Yang, H., Antoine, D.J., Andersson, U. & Tracey, K.J. The many faces of HMGB1: molecular structure-functional activity in inflammation, apoptosis, and chemotaxis. *J. Leukoc. Biol.* **93**, 865–873 (2013).
49. Shin, H.J. *et al.* Kinetics of binding of LPS to recombinant CD14, TLR4, and MD-2 proteins. *Mol. Cells* **24**, 119–124 (2007).
50. Scaffidi, P., Misteli, T. & Bianchi, M.E. Release of chromatin protein HMGB1 by necrotic cells triggers inflammation. *Nature* **418**, 191–195 (2002).
51. Brochu, C. *et al.* NF-κB–dependent role for cold-inducible RNA binding protein in regulating interleukin 1β. *PLoS ONE* **8**, e57426 (2013).

ONLINE METHODS

Human blood specimens. Blood samples were obtained from patients admitted to the surgical ICU at North Shore University Hospital and Long Island Jewish Medical Center. Serum was separated and stored in aliquots at −80 °C. Informed consent was obtained from all participants, and human subject protocols were approved by the Institutional Review Board of the North Shore–Long Island Jewish Health System.

Experimental animals. Male Sprague-Dawley rats (Charles River, Wilmington, Massachusetts), weighing 275–325 g, were used in the experiments. *Cirbp*$^{-/-}$ mice with a C57BL/6 background were provided by Kumamoto University, Japan[52]. *Ager*$^{-/-}$, *Tlr2*$^{-/-}$ and *Tlr4*$^{-/-}$ mice were described previously and were maintained at the Feinstein Institute for Medical Research[47]. C57BL/6 WT mice were purchased from Jackson Laboratory (Bar Harbor, Maine). Male and age-matched (10–12 weeks of age) mice were used in the experiments. Animals were randomly assigned to the sham, vehicle control or treatment groups. The number of animals used in each group was based on our previous publications[53,54] on animal models of hemorrhage and sepsis. Not all animal studies were conducted in a completely blinded fashion. Animals were excluded from the analysis if they died during the surgical operation. All experiments were performed in accordance with the guidelines for the use of experimental animals by NIH (Bethesda, Maryland) and were approved by the Institutional Animal Care and Use Committee (IACUC) at the Feinstein Institute for Medical Research.

Animal model of hemorrhagic shock. Animals were anesthetized with isoflurane inhalation. Catheters (PE-50 tubing) were placed in both the femoral veins and arteries. The animal was bled to a mean arterial pressure of 25–30 mm Hg within 10 min. This pressure was maintained for 90 min, and then animals were resuscitated with lactated Ringer's solution (the equivalent of two times the maximum bleed-out volume) over a 60-min period. Sham-operated animals underwent the same surgical procedure without bleeding and resuscitation.

Animal model of polymicrobial sepsis. Animals were anesthetized with isoflurane inhalation. CLP was performed through a midline laparotomy. Briefly, a 2-cm midline abdominal incision was performed. The cecum was exposed, ligated just distal to the ileocecal valve to avoid intestinal obstruction, punctured twice with an 18-gauge needle, squeezed slightly to allow a small amount of fecal matter to flow from the holes and then returned to the abdominal cavity. The abdomen was closed in layers with suture. Sham-operated animals underwent the same procedure with the exception that the cecum was neither ligated nor punctured. The animals were resuscitated with 3 ml per 100 g body weight normal saline subcutaneously immediately after surgery.

Cell culture and isolation of peritoneal macrophages. Mouse macrophage-like RAW 264.7 cells and human monocyte THP-1 cells were obtained from ATCC (Manassas, Virginia). Primary peritoneal macrophages were isolated from C57BL/6 WT, *Ager*$^{-/-}$, *Tlr2*$^{-/-}$ and *Tlr4*$^{-/-}$ mice at day 3 after intraperitoneal injection with 4% thioglycolate as described previously[47]. Rat primary peritoneal macrophages were isolated directly from the abdominal cavity of a male Sprague-Dawley rat without preinduction. RAW 264.7 cells and peritoneal macrophages were cultured in DMEM and RPMI 1640 (Invitrogen, Grand Island, New York), respectively. THP-1 cells were cultured in RPMI 1640 with 0.05 mM β-mercaptoethanol and differentiated into macrophage-like cells by incubating with phorbol 12-myristate 13-acetate (20 ng m^{-1}) for 48 h. All cultured media were supplemented with 10% heat-inactivated FBS, 1% penicillin-streptomycin and 2 mM glutamine. Cells were maintained in a 37 °C incubator with 5% CO_2.

Isolation of human PBMCs. Human PBMCs were isolated from blood obtained from healthy donors at the New York Blood Bank by centrifugation over a Ficoll-Paque Plus (GE Healthcare, Port Washington, New York) density gradient according to standard protocols. Isolated cells were washed with RPMI 1640 complete medium and cultured on a plate. After 2 h, the nonadherent cells were removed, and the adherent cells were cultured overnight before use.

Administration of rmCIRP and antisera to CIRP. One milliliter of rmCIRP or normal saline (vehicle) was administered intravenously to healthy animals. Antisera to CIRP, rabbit control IgG or vehicle was administered to hemorrhaged rats 15 min after the initiation of fluid resuscitation over a period of 45 min through the femoral venous catheter.

Survival study. The hemorrhaged rats were administered antisera to CIRP, rabbit control IgG or normal saline (vehicle) for 3 consecutive days, and survival was monitored for 10 d. WT and *Cirbp*$^{-/-}$ mice were subjected to hemorrhage, and survival was recorded for 72 h. The septic rats were administered antisera to CIRP or rabbit control IgG at 5 h after CLP. Necrotic cecum was removed 20 h after CLP, and survival was monitored for 10 d.

RT-PCR assay. Total RNAs were extracted by TRIzol (Invitrogen). The cDNA was synthesized using MLV reverse transcriptase (Applied Biosystems, Grand Island, New York). PCR reactions were performed in QuantiTect SYBR Green PCR mixture (Qiagen, Valencia, California) and analyzed by the Applied Biosystems 7300 PCR System. GAPDH was used as an internal control for normalization, and the relative expression level of the analyzed gene was calculated by the ΔΔCt method. Each sample was measured in duplicates. The RT-PCR primers were synthesized from Operon (Huntsville, Alabama). The primer sequences were as follows: rat CIRP (NM_031147), 5′-GGGTCCTACAGAGACAGCTACGA-3′ (forward), 5′-CTG GACGCAGAGGGCTTTTA-3′ (reverse); TNF-α (NM_012675), 5′-CCC AGACCCTCACACTCAGA-3′ (forward), 5′-GCCACTACTTCAGCATC TCG-3′(reverse); and GAPDH (NM_017008), 5′-ATGACTCTACCCACGGC AAG-3′ (forward), 5′-CTGGAAGATGGTGATGGGTT-3′ (reverse).

Western blot analysis. Tissue samples were homogenized in RIPA buffer (10 mM Tris-HCl, pH 7.5, 120 mM NaCl, 1% NP-40, 1% sodium deoxycholate and 0.1% SDS) containing a protease inhibitor cocktail (Roche, Indianapolis, Indiana). Protein concentration was determined by a DC protein assay (Bio-Rad, Hercules, California). Equal amounts of serum or tissue homogenates were fractionated by SDS-PAGE and transferred to a nitrocellulose membrane. The membrane was incubated with antibodies to CIRP (1:100; 10209-2-AP; ProteinTech, Chicago, Illinois), GAPDH (1:1,000; sc-25778; Santa Cruz, Santa Cruz, California), histone (1:1,000; 9715; Cell Signaling, Danvers, Massachusetts), BAX (1:1,000; sc-526; Santa Cruz), actin (1:10,000; A5441; Sigma-Aldrich, St. Louis, Missouri), cathepsin D (1:1,000; sc-10725; Santa Cruz) or HMGB1 (1:500; ab18256; Abcam, Cambridge, Massachusetts), followed by a secondary antibody–horseradish peroxidase conjugate (1:10,000; SouthernBiotech, Birmingham, Alabama), and developed with a chemiluminescence detection kit (GE Healthcare). Band intensities were quantified with densitometry.

Determination of cytokine levels. TNF-α and IL-6 concentrations in serum, tissue homogenates and culture media grown with macrophages were measured by ELISA kits from BioSource (Camarillo, California). HMGB1 levels were determined by western blotting.

Measurements of transaminases and myeloperoxidase activity. Serum concentrations of AST and ALT were determined by assay kits from Pointe Scientific (Canton, Michigan). To determine myeloperoxidase activity, liver tissues were homogenized in 50 mM phosphate buffer (pH 6.0) containing 0.5% hexadecyltrimethylammonium bromide. After centrifugation, supernatant was added to the reaction solution (0.2 mg ml^{-1} O-dianisidine dihydrochloride and 0.2 mM H_2O_2 in phosphate buffer), and change of optical density at 460 nm per min was recorded to calculate the activity.

***In vitro* hypoxia.** Hypoxia was produced using a sealed chamber containing 1% O_2, 5% CO_2 and 94% N_2 placed in an incubator at 37 °C. The culture medium was changed to Opti-MEM I medium (Invitrogen) before subjecting cells to hypoxic conditions. After 20 h incubation in the hypoxic chamber, cells were then cultured at normal culture condition for different time periods and collected for further analyses.

Cell fractionation. For isolation of nuclear and cytoplasmic fractions, RAW 264.7 cell pellets were resuspended in buffer containing 10 mM 4-(2-hydroxyethyl)-1-piperazineethanesulfonic acid (HEPES) and KOH, pH 7.9, 1.5 mM $MgCl_2$, 10 mM KCl, 0.5 mM dithiothreitol and a protease inhibitor cocktail on

doi:10.1038/nm.3368

ice for 15 min. After centrifugation, the supernatant was collected as the cytoplasmic fraction, and the pellet was resuspended in buffer containing 20 mM HEPES and KOH, pH 7.9, 25% glycerol, 420 mM NaCl, 1.5 mM $MgCl_2$, 2 mM EDTA, 0.5 mM dithiothreitol and a protease inhibitor cocktail on ice for 20 min. After centrifugation, the supernatant was collected as the nuclear fraction. The isolation of lysosomes was performed with a Lysosome Enrichment Kit as instructed by Thermo Scientific (Waltham, Massachusetts).

Expression of the GFP-CIRP fusion protein. The construction of the GFP-CIRP expression plasmid was described previously[21]. RAW 264.7 cells were transfected with the plasmid using Lipofectamine reagent (Invitrogen). Cells were also transfected with a GFP expression plasmid alone as a control for comparison.

Determination of CIRP release in serum and cultured cells. The conditioned medium from normoxic or hypoxic plus reoxygenated RAW 264.7 cells was incubated with 0.02% deoxycholic acid and 10% trichloroacetic acid at 4 °C overnight for protein precipitation, and it was then subjected to western blotting. Lactate dehydrogenase activity was determined by an assay kit from Pointe Scientific. Serum CIRP concentration was estimated using serial dilutions of purified CIRP as a standard on western blot analysis.

Recombinant proteins. rmHMGB1 was produced as described previously[32]. Recombinant rat TNF-α was obtained from Biosource. rhCIRP (NP_001271; full length) with a C-terminal DDK tag was transfected and expressed from human HEK293 cells and obtained from Origene (Rockville, Maryland). rhTLR2 (NP_003255; Glu21–Leu590) and rhTLR4 (O00206; Glu24–Lys631) were transfected and expressed from the mouse myeloma NS0 cell line. rhMD2 (BAA78717; Glu17–Asn160) was transformed and expressed from *Escherichia coli*. The rhTLR4-MD2 complex was purified from NS0 cells that coexpressed rhTLR4 (O00206; Glu24–Lys631) and rhMD2 (Q9Y6Y9; Glu17–Asn160) with a histidine (His) tag at each protein. All rhTLR2, rhTLR4 and rhMD2 were fused with a 10-His tag at their C terminus and were obtained from R&D Systems (Minneapolis, Minnesota). rhRAGE (Q15109; Ala23–Ala344) with a C-terminal 6-His tag was transfected and expressed from human HEK293 cells and obtained from Biovision (Milpitas, California).

Synthesis of oligopeptides. A panel (32 total) of 15-mer oligopeptides with five-amino-acid offsets across the entire human CIRP sequence was synthesized at Genscript (Piscataway, New Jersey). All Fmoc-protected amino acids, solvents, TBTU and 2-chlorotrityl (2-Cl⁻Trt) resin were purchased from Sigma-Aldrich. The synthesis of oligopeptides was carried out using a Fmoc/tBu solid-phase peptide synthesis (SPPS) strategy on a Tetras automated peptide synthesizer (Creosalus, Louisville, Kentucky). The SPPS protocol consisted of two consecutive deprotection steps and a coupling step. The synthesis was performed on 2-Cl⁻Trt resin. The crude peptide was precipitated, washed and lyophilized. The purification of the crude peptide was performed by semipreparative reversed-phase HPLC. The peptide was identified by electrospray ionization mass spectrometry analysis.

SPR analysis. Analysis of protein-protein and peptide-protein interactions was conducted using the BIAcore T200 instrument (GE Healthcare). Binding reactions were performed in 1× PBS buffer containing 0.01% Tween-20 (pH 7.4). The CM5 dextran chip (flow cell-2) was first activated by injection with 89 µl of 0.1 M N-ethyl-N′-[3-diethylaminopropyl]-carbodiimide and 0.1 M N-hydroxysuccinimide. An aliquot of 200 µl of 5 µg ml^{-1} of the ligand diluted in 10 mM sodium acetate (pH 4.5) was injected into flow cell-2 of the CM5 chip for immobilization. Next, 135 µl of 1 M ethanolamine (pH 8.2) was injected to block the remaining active sites. The flow cell-1 without coating with the ligand was used as a control to evaluate nonspecific binding. The binding analyses were performed at a flow rate of 30 µl min^{-1} at 25 °C. To evaluate the binding, the analyte (ranging from 62.5 nM to 1.0 µM for the kinetics analysis or 0.5 µM for the yes-or-no binding analysis) was injected into flow cell-1 and flow cell-2, and the association of analyte and ligand was recorded by SPR. The signal from the blank channel (flow cell-1) was subtracted from the channel coated with the ligand (flow cell-2). Data were analyzed by the BIAcore T200 Evaluation Software. For all samples, a blank injection with buffer alone was subtracted from the resulting reaction surface data. Data were globally fitted to the Langmuir model for 1:1 binding.

Construction of the CIRP expression plasmid. Rat CIRP cDNA (NM_031147) was synthesized from total RNA isolated from rat hearts by using MLV reverse transcriptase with oligo $d(T)_{16}$ primers. The cDNA was amplified with the oligonucleotide primers sense, 5′-CACCATGGCATCAGATGAAGG-3′ and antisense, 5′-CTCGTTGTGTGTAGCATAGC-3′. The resulting PCR product was digested with EcoRV and NotI and cloned into the pENTR vector (Invitrogen) at the C terminus of the hexahistidine tag and then transformed to *E. coli* BL21 (DE3). Individual clones were selected by kanamycin resistance.

Purification of rmCIRP. Transformed *E. coli* carrying the rat His-CIRP expression plasmid were inoculated in Luria-Bertani medium containing kanamycin overnight and induced with 1.0 mM isopropyl β-D-1-thiogalactopyranoside for another 6 h. The bacteria were harvested by centrifugation, and the pellet was washed once with 20 mM Tris-HCl, pH 7.9. The bacterial pellet was resuspended in buffer containing 20 mM Tris-HCl, pH 7.9, 500 mM NaCl and 5 mM imidazole and lysed by sonication at 4 °C. The soluble extract was clarified by centrifugation at 20,000*g* at 4 °C for 1 h. The clear lysate was loaded onto a nickel–nitrilotriacetic acid (Ni^{2+}-NTA) column (Novagen, Madison, Wisconsin). The bound protein was washed with 20 mM Tris-HCl, pH 7.9, 500 mM NaCl and 100 mM imidazole and was eluted in the same buffer supplemented with 1.0 M imidazole. All proteins were dialyzed with PBS and stored at −80 °C for further analysis.

Removal of LPS from the purified rmCIRP preparation. Triton X-114 (Sigma-Aldrich) was added to the purified protein solution to a final concentration of 5%. The mixture was rotated at room temperature for 15 min to ensure a homogenous solution. Then the mixture was centrifuged at 14,000*g* for 12 min. The upper aqueous phase containing rmCIRP (free of LPS) was carefully removed. The level of LPS in the removed solution was measured by a Limulus amebocyte lysate (LAL) assay (Cambrex, East Rutherford, New Jersey).

Validation of the purified rmCIRP. The purity of the rmCIRP preparation was examined by SDS-PAGE staining with Coomassie blue, which showed a major band at 24 kDa and very minor bands at other positions (**Supplementary Fig. 3a**). The identity of rmCIRP was further confirmed by western blotting against antibodies to CIRP from two different sources, one generated from our laboratory and the other from ProteinTech (**Supplementary Fig. 3b**). The purified rmCIRP was further validated by amino acid sequence analysis using liquid chromatography tandem mass spectrometry at the Proteomics Resource Center of the Rockefeller University, New York. The recombinant protein was identified as CIRP with >95% confidence using the MASCOT database search algorithm.

Production of antisera to CIRP. Antisera against the purified rmCIRP were raised in New Zealand White rabbits by standard procedures at Covance (Princeton, New Jersey). The IgG fraction was isolated from the antisera by immobilized immunopure protein-A and -G chromatography (Pierce). The specificity of the antisera to CIRP was examined by western blotting against its purified protein. LPS was undetectable in the antiserum preparations, as measured by LAL assay (Cambrex). The same process was performed to purify rabbit serum control IgG.

Statistical analyses. Numerical data are expressed as the mean ± s.e.m. and were compared by one-way ANOVA and Student-Newman-Keuls test. Student's *t* test was used for two-group analyses. The majority of the data sets passed the normality test. Some data sets had a statistical difference in the variation between groups. The survival rate was estimated by the Kaplan-Meier method, and rates were compared using the log-rank test. Differences in values were considered significant at $P < 0.05$.

52. Sakurai, T. *et al.* Cirp protects against tumor necrosis factor-α–induced apoptosis via activation of extracellular signal-regulated kinase. *Biochim. Biophys. Acta* **1763**, 290–295 (2006).
53. Wu, R. *et al.* Mechanisms responsible for vascular hyporesponsiveness to adrenomedullin after hemorrhage: the central role of adrenomedullin binding protein-1. *Ann. Surg.* **242**, 115–123 (2005).
54. Miksa, M. *et al.* Immature dendritic cell–derived exosomes rescue septic animals via milk fat globule epidermal growth factor-factor VIII. *J. Immunol.* **183**, 5983–5990 (2009).